Longwall Gateroad Stability Analysis Based on Field Monitoring and Bonded Block Modeling Results

Zoheir Khademian
CDC NIOSH, Pittsburgh Mining Research Division, Pittsburgh, PA

Gabriel S. Esterhuizen, and

Morgan Sears
CDC NIOSH, Pittsburgh Mining Research Division, Pittsburgh, PA

ABSTRACT
Based on the 2010-2019 Mine Safety and Health Administration (MSHA) accident report database, 91% of reported ground control accident in the US longwall mines were caused by gateroad roof instability. This can be related to the significant changes in loading conditions that gateroads are subject to from the development to the longwall abutment loading phases, combined with the thinly bedded shale roof, found in many US longwall coal mines. One of the challenges in designing efficient support systems is to understand the roof instability mechanisms along with support-roof interactions under this complex loading condition. Field monitoring of roof displacement and stress changes coupled with detailed analyses using numerical models are well-documented techniques to study the causes of roof instabilities. However, traditional modeling techniques require additional calibration to simulate delamination and buckling of shale roof, one of the main roof instability mechanisms in longwall mines. One alternative modeling technique is the UDEC Bonded Block Method (BBM) where bedded roof and support interactions can be explicitly captured. This paper presents the development of a BBM model of a longwall entry at a 180 m depth of cover with a three-entry gateroad layout along with roof extensometer monitoring results. The models are validated against the monitoring data, showing the potential for BBM numerical models capturing the complex roof and support system interactions to assist with optimizing gateroad layouts and support systems.

INTRODUCTION
Longwall gateroad entries experience significant variations in the loading condition from the development to the longwall abutment loading phase. The wide variation of stress magnitudes and orientations coupled with the geology of thinly bedded shale roof contribute to the challenge of the support system design in gateroad entries. Currently the design of support systems for gateroads in the US longwall mines is based on local experience or in-mine trials. However, the need for improving the support design procedures is well reflected in the MSHA database. From 2010 to 2019, roof falls accounted for 91% of total ground control accidents, 78% of the ground control injuries, and 36% of ground control fatalities in the US underground coal mines (Rashed, et al. 2022).

Numerical models validated by ground-truth roof monitoring results are useful tools for understanding the roof response to the stress variation and designing effective support systems. However, traditional continuum models are inherently limited when the instability is caused by delamination and buckling of rock layers, two main prominent failure mechanisms of thinly bedded shale roofs in longwall mines (Hasenfus and Su 2006). Thus, as shown by Tulu et al. (2016) and Esterhuizen (2012), the constitutive models used in continuum models must be modified to improve their ability to capture the complex ground response and interactions between support and the rock material. Esterhuizen et al. (2019) used a combined brittle/shear mechanism and realistically simulated the strength anisotropy and delamination of bedded strata. While the current approach for modeling the roof response remains valid, relatively new discontinuum modeling techniques such as BBM are expected to more closely represent the mechanical response of rock and its interaction with the support systems. This is mainly because BBM allows for initiation, coalescence, and propagation of shear and tensile fractures within rock units leading to roof collapse (Gao and Stead 2014). However, the applicability of the BBM-based models for entry roof stability analyses needs to be confirmed through field measurements and case studies.

This paper presents the latest efforts in an ongoing research program in National Institute for Occupational Safety and Health (NIOSH) to develop validated numerical models of supported entries and the surrounding rockmass that can be used to evaluate support alternatives (Esterhuizen, et al. 2019). The hypothesis is that with the use of BBM approach, the delamination failure and buckling mechanisms can be successfully simulated with no need for additional calibration for assigning different strengths in vertical and lateral directions. In this paper, BBM techniques in Universal Distinct Element Code (UDEC) are evaluated by a series of field-scale confined compressive test models (1m by 2m) and then are used to model a longwall gateroad entry roof.

The validation data for the model development are a series of field studies where ground and support responses in an active gateroad were monitored. The monitoring site is in a longwall mine in the eastern US, mining the lower Kittanning coal bed at a depth of cover of 150 m to 240 m (Esterhuizen et al. 2017). Rock strengths and in-situ stresses were determined by laboratory tests and field measurements. The developed BBM approach is applied, and the results are compared to demonstrate the benefits of the BBM modeling technique.

METHODOLOGY

The BBM technique implemented in UDEC models rock as an assembly of smaller blocks with polygonal (Voronoi) or triangular (trigon) shapes, bonded together at their contacts with cohesion and tensile strengths. The contacts' normal and shear stiffnesses, cohesion, and tensile strengths are known as the micro mechanical properties that together with the block material properties determine the macro mechanical property of the assembled rock unit. The blocks themselves can be treated as elastic or non-linear materials.

This paper uses two-dimensional elastic trigons with contacts that follow a Mohr-Coulomb constitutive behavior with residual cohesion. A calibration process is adopted to obtain the micro mechanical properties (normal and shear stiffnesses, cohesion, and friction) of the trigon's contact that represents the macro mechanical properties (elastic modulus, tensile strength, internal friction, and cohesion) of each rock unit. Then, a set of field-scale numerical confined compressive tests are conducted to evaluate the BBM technique in representing the strength variations of thinly bedded rock specimens under different stress orientations. A detailed-scale model of the gateroad entry in the study mine was constructed with and without the support systems. The boundary conditions on the entry model after the development phase were obtained from field monitoring results supplemented by a panel-scale numerical model of the study mine discussed by Esterhuizen et al. (2019).

The development phase was modeled by removing materials within the boundaries of the modeled entry and then gradually relaxing traction on the excavated boundaries in ten decremental loading steps. The support systems in the supported entry model are installed at the seventh step in the unloading process, assuming the last unloading step represents the completion of the development phase.

The question of what constitutes a roof collapse in a numerical model is addressed by recording the velocity of the entry roof in different stages of mining. So, roof is considered failed when the roof slabs are accelerating (increasing velocity) under constant boundary loading conditions. The model is considered validated when the displacement of different units in the roof after support installation are close to the extensometer measurements conducted in the study site.

STRENGTH OF THINLY BEDDED ROCK SPECIMEN

A set of confined compressive numerical tests were conducted to evaluate BBM models that represent a portion of a thinly bedded shale roof. The specimens are 2 by 1 m and are bedded by a set of joints with 0.1 m spacing. This configuration is assumed to represent roof strata consisting of 0.1-m-thick slabs. The bedding angle is varied in 10-degree increments to evaluate the reduction of strata strengths with stress orientations. The confinement stress of

5 MPa, 4 MPa, and 3 MPa, and zero are applied and thus UCS, cohesion, and internal friction of each specimen are recorded. The input parameters for trigon's contacts are shown in Table 1, calibrated to represent a shale specimen with the intact rock UCS of 12 MPa and Young's modulus of 6 GPa (Zipf 2006). The bedding planes are assigned a cohesion of 0.1 MPa and a friction of 30 degrees. The residual cohesion of beds reduces to 0.01 MPa once slip is initiated.

Table 1. Trigon's micromechanical properties for confined compressive tests

Trigons micro mechanical contact properties	Values
Normal stiffness	1.6 e12 N/m
Shear stiffness	6.4 e11 N/m
Cohesion	5 MPa
Residual cohesion	0.5 MPa
Friction	26 degrees
Residual friction	26 degrees
Tensile strength	2.1 MPa
Residual tensile strength	0
Intact rock elastic modulus	10 GPa
Intact rock Poisson ratio	0.3

Figure 1 shows the tensile (red) and shear fractures (blue) developed during each test with zero confinement (UCS) along with the trigon boundaries shown in green. Failure mechanisms vary from slip along the beddings to tensile cracks along trigon contacts in the intact rock. The corresponding results for cohesion, internal friction angle, and UCS are plotted in Figure 2.

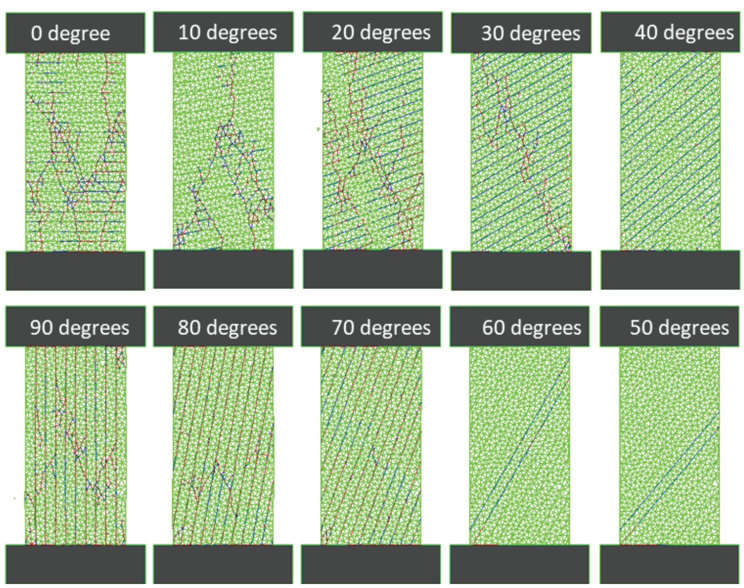

Figure 1. UCS specimen with different bedding angles showing fracture propagation and failure mechanisms. Tensile fractures are red and shear fractures are blue. Trigons are shown in green.

The UCS of specimens with vertical (90 degrees) and horizontal (0 degree) beddings are the closest to the intact shale with UCS 12 MPa. However, UCS reduces to the bedding plane cohesion of 0.1 MPa when the bedding angle is around 60 degrees, close to the failure plane of 45+25/2 degrees. Confined compressive tests are conducted with the confinement stress of 3, 4, and 5 MPa.

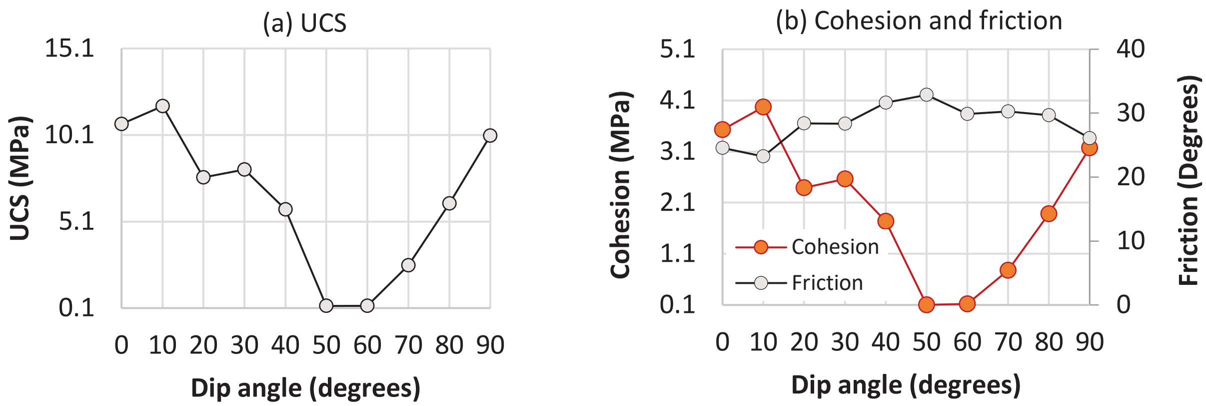

Figure 2 (a) UCS, and (b) cohesion and friction evolution with varying lamination orientation.

The cohesion and friction angle for each specimen is calculated and plotted in Figure 2b. A reduction in the rock cohesion to the bedding plane cohesion values is observed around bedding angle of 60 degrees. The friction, however, stays almost constant between 25 to 30 degrees. The results so far confirm that BBM can be used to model intact rock and that BBM interactions with bedding planes can reasonably simulate the reduction of bedded shale strength under different stress orientations (Huang, et al. 2019).

DESCRIPTION OF MINE SITE

The selected longwall mine is located in the eastern US and extracts the lower Kittanning coal bed with 152 m to 243 m of cover. The longwall panels are 365 m wide with a mining height of approximately 2.1 m, and entry development height up to 2.4 m. The study site is in the tailgate of the third panel to be mined in the district. The monitoring site was part of a three-entry gateroad system that serves the two longwall panels referred to as the first and second panel in this paper as shown in Figure 3.

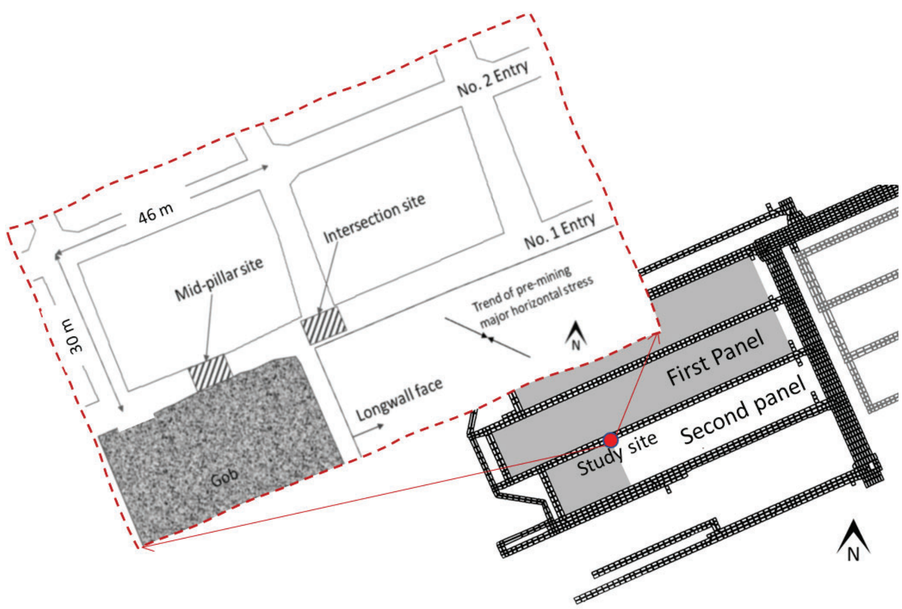

Figure 3. Pillar layout and monitoring site location at the longwall mine selected for this study.

The monitored entry serves as the tailgate of the second panel. Entry and crosscut developments are 5.5 m wide. Monitoring was initiated a few days after development of the gateroad entries and continued during passage of the longwall panels on either side of the monitoring site. Figure 3 shows the details of the pillar layout, the longwall face, and the location of the monitoring site on the last day of monitoring when the second panel mined by the monitoring site. The ground overburden depth was close to 180 m at the locations of the instruments.

GEOTECHNICAL SETTING

The general overburden consists of alternating sandstone and shale beds with sandstone layers between 9-m and 18-m thick. The immediate roof of the entries in Lower Kittanning coalbed ranges from dark gray to carbonaceous clay shale. The Johnstown limestone is located above this sandy zone and locally grades laterally to a claystone. Table 2 summarizes the strength and mechanical properties of the rocks within the immediate roof. Following Esterhuizen et al. (2013), the Coal Mine Roof Rating (CMRR) (Molinda and Mark 1994) is used to estimate the large-scale field strength of the strata.

Table 2. Key rock properties at the study site

Rock type	Elastic modulus (GPa)	Friction angle (degrees)	Cohesion (MPa)	Tensile strength (MPa)
Limestone	50	30	34	11
Gray clay shale	8	28	6	2
Clay shale	10	28	7	2
Carbonaceous shale	15	28	11	4
Shaley sandstone	18	38	10	3

Figure 4 shows the UDEC model geometry with the actual roof composition given by the core drilling at the instrumentation site. The roof at the modeled cross section was monitored by three extensometers each 2.4-m long (No. 1, No. 2, and No. 3) and a single 6-m-long roof extensometer (No. 5). The installation locations of the extensometers are shown on the UDEC model in Figure 4.

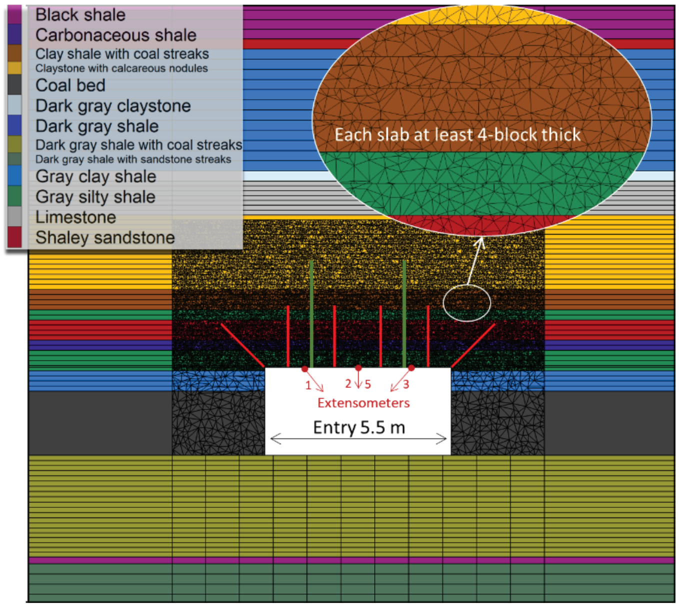

Figure 4. Lithology profile of the roof and floor at the monitoring site along with the support system, and trigons geometry and density.

Overcore stress measurements conducted at the instrumentation site showed that the major horizontal stress was 7.6 MPa oriented at N80W, and the minor horizontal stress was 5.9 MPa. The main development directions of the mine are oriented at about 45° to the major horizontal stress (Figure 3). Thus, the headgate entries are located in a horizontal stress relief zone while the tailgate is exposed to unfavorable stress concentrations. Detailed discussions on the monitoring results and analysis of the entry response were published by (Gearhart, et al. 2017). Here, only roof displacements at four points across the entry are presented at the end of the monitoring period and compared with the UDEC results. This is because models only predict reasonable roof displacement if rock mass, loading conditions, and support systems are all modeled with sufficient realism.

SUPPORT SYSTEMS

The primary roof support consisted of rows of four fully grouted roof bolts (1.8 m by 19.1 mm) spaced on 1.2 m centers (Figure 4). The secondary support was a pair of cable bolts (3 m by 15 mm) with 1.2 m of resin grout anchorage installed through a strap every 2.4 m. Secondary support was installed about 18.2 to 30.4 m outby the advancing face during retreating. In addition, there were fully grouted bolts installed at a 45-degree angle at the corner of the rib and roof on 2.4 m spacing. The standing support system was also used to ensure stable ground conditions up to the advancing longwall face and to provide an adequate opening along the edge of the gob. Standing supports in the form of two rows of nine-point wooden cribs were installed in the mine but they are not considered in the models here because from crib load measuring devices, the supports did not carry noticeable loads until after the second panel was mined by the monitoring site.

NUMERICAL MODELING

The limiting factor in running numerical models and understanding detailed behavior of rock under complex stress conditions is the computation time. In particular, to fully benefit from the BBM models of thinly bedded rock units, trigons in the scale of centimeters should be modeled but this level of detail requires prohibitive computation time for full-scale modeling of longwall mines with hundreds of meters in each dimension. One well-documented approach is to find stress boundary conditions for an isolated area within a low-resolution panel-scale model and then use the boundary conditions in an entry-scale model with a high level of resolution (finer mesh or trigons).

Entry loading condition by panel-scale model

The results of a panel-scale 3D model constructed earlier by Tulu et al. (2018) to approximate stresses around gateroad entries was used here to inform boundary condition of the entry-scale models. The panel scale model included 61 geologic layers up to the surface with element size of 1-10 m. The modeling procedures and selection of input properties for the panel-scale model are based on previous investigations by Esterhuizen et al. (2010) and Tulu et al. (2017). Results from the panel-scale models with the actual longwall panel layout, consisting of 456-m-wide panels and three gateroad entries are presented in Figure 5, showing the maximum horizontal stress distribution around the longwall panels and the location of the monitoring sites at the end of the monitoring period. Tulu et al. (2018) compared the ground subsidence, the extent of abutment stress around the longwall panel, and stress magnitudes in and around the gateroad pillars with field measurements and showed that the model provides reasonable estimates of ground response.

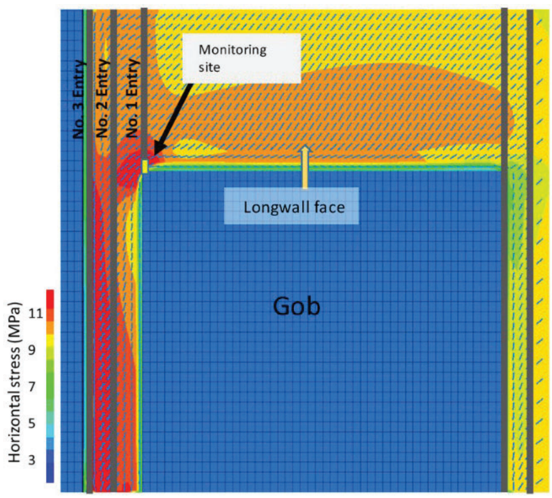

Figure 5. Maximum horizontal stress distribution and orientation 3 m above the mined coal bed in the panel-scale model (after Esterhuizen, et al. 2019).

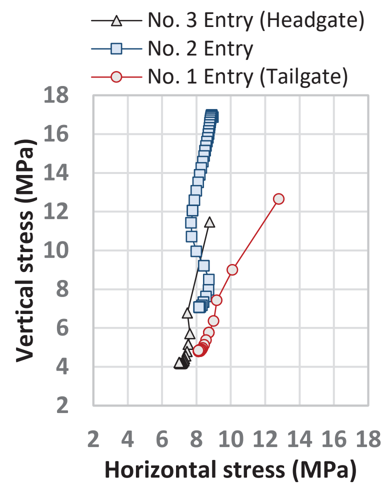

Figure 6. Stress path experienced by three entries in the model in vertical plane perpendicular to the long axis of the entry (Esterhuizen, et al. 2019)

Figure 6 shows the modeled gateroad loading paths recorded as the vertical and horizontal stresses above the roof line at different face locations. The stress values are recorded in the panel-scale model 3 m above the roof line. Each marker on the curves represents a 9-m advance of the longwall face. The initial stress state in the model is with the horizontal stress of 7.1 MPa and vertical stress of 4.2 MPa. The highest stress point on the curves shows where the second panel face mined by the monitoring location. The stress path of the No. 1 (tailgate) entry shows a higher increase in horizontal stress compared to the other two entries. After the second panel mined by the monitoring site in the model, the vertical stress and horizontal stress at this location were 12.8 and 12.7 MPa, respectively. The change in stresses was also recorded at the field monitoring site by hollow-inclusion stress cells, showing that the vertical and horizontal stress values 8 m above the tailgate entry roof were 10.3 MPa and 11.5 MPa, respectively, at the end of the monitoring period. The results of the panel-scale numerical model are in reasonable agreement with the measured values at the site. With this confirmation, this No. 1 entry stress path obtained from the model (Figure 6) is applied as the boundary conditions of BBM entry-scale models in the following section.

Models of Entry Response

BBM trigon blocks were constructed only 5 m above the roof line because there is a direct relationship between the number of blocks in a model with the runtime. For the same reason, 3 m of ribs are constructed with trigons with larger edges (0.2 m). The edge of trigons above the roof line varies according to thickness of each slab so that at least four trigons are located across each slab.

As shown in Figure 4, UDEC BBM models were created to represent the detailed geology, entry dimensions, and support systems at the monitoring site. The entry-scale model is two dimensional, simulating a vertical slice through the entry No. 1. In total, 92 bedding planes in the roof and floor are modeled. Up to 5 m above the roof line, 35 slabs each 10 to 20 cm thick are modeled. Each slab is made up of trigon with an edge size ranging from 2 to 6 cm. Each slab is made at least four-trigon thick. The entire model, including the trigon blocks, are discretized, and made deformable. The rib response was not of interest here so larger trigon blocks with less resolution (20-cm edge size) are used to construct the ribs. The possible effects of rib failure on roof stability will be studied in future works.

Calibration

All materials in the model are elastic with properties listed in Table 2 for different units but the trigon contacts can fail under excessive stress. The micro mechanical properties of the trigon block contacts in each slab are calibrated to represent the macro mechanical properties in Table 2 except for the dilation angle that is considered constant at 10 degrees for all bedding planes and trigon contacts. Micro mechanical properties of the trigon block contacts in each slab are calibrated with a given seed number as different realization of trigons may lead to different macro mechanical response.

Mining process

The No. 1 entry model in Figure 4 is initially solved under in-situ pre-longwall mining loading conditions with 4.2 MPa of vertical stress and 7.1 MPa of horizontal stress. The model material in the entry is removed and counteracting forces are applied on the entry boundary. The forces are then gradually reduced to zero in ten steps to simulate gradual development of the entry. For simulating the effects of the first and second panel mining, the loadings on the boundary of the model is increased following the stress path in Figure 6 for No. 1 entry. The horizontal loads are increased by velocity loading applied to the left and right boundaries. The vertical loads are increased directly by applying stresses on the top boundary of the model while the bottom boundary is fixed by rollers.

The model at the final loading condition that represents the second panel passing the monitoring site is used for the comparison with the measured roof displacements. Two sets of models are constructed to investigate failure mechanisms and roof response. The first set is to study roof response and the second set is for studying the role of support systems, each being separately discussed at the entry development stage and once the second panel reaches the cross section being modeled (monitoring site).

MODELING RESULTS

Entry Model Response without support

Figure 7 shows the entry model response after the entry boundary is fully unloaded or in other words the entry is fully developed without the support system in place. Figure 7a shows tensile fractures in red and shear fractures highlighted in cyan. Tensile and shear fractures delaminate the roof driven by the buckling failure mechanism. Figure 7b shows vertical roof sagging with large displacement in the few first slabs above the roof line. The horizontal stress in the model is shown in Figure 7c showing the low values in the first few slabs above the roof line, but the failure height is not clear. Figure 7d shows the vertical velocity plot that shows only one delaminated slab is collapsing and the roof is generally stable under the development loading conditions. Figure 8 shows the model predicted entry response up to the second panel passing the monitoring site without the support system in place. As shown in Figure 8a, tensile fractures are concentrated at the corners and the center of the roof. Figure 8b shows how thinly bedded shale roof is delaminated into individual slabs. The slabs fail by buckling or shear failures and progressively induce failure upwards due to the reduced confinement. Figure 8c shows how the horizontal stress is transferred from lower delaminated slabs to the stronger sandstone beds about 1.6 m above the roof line. Figure 8d shows clearly that the roof is collapsing with an increasing velocity of the failed slabs.

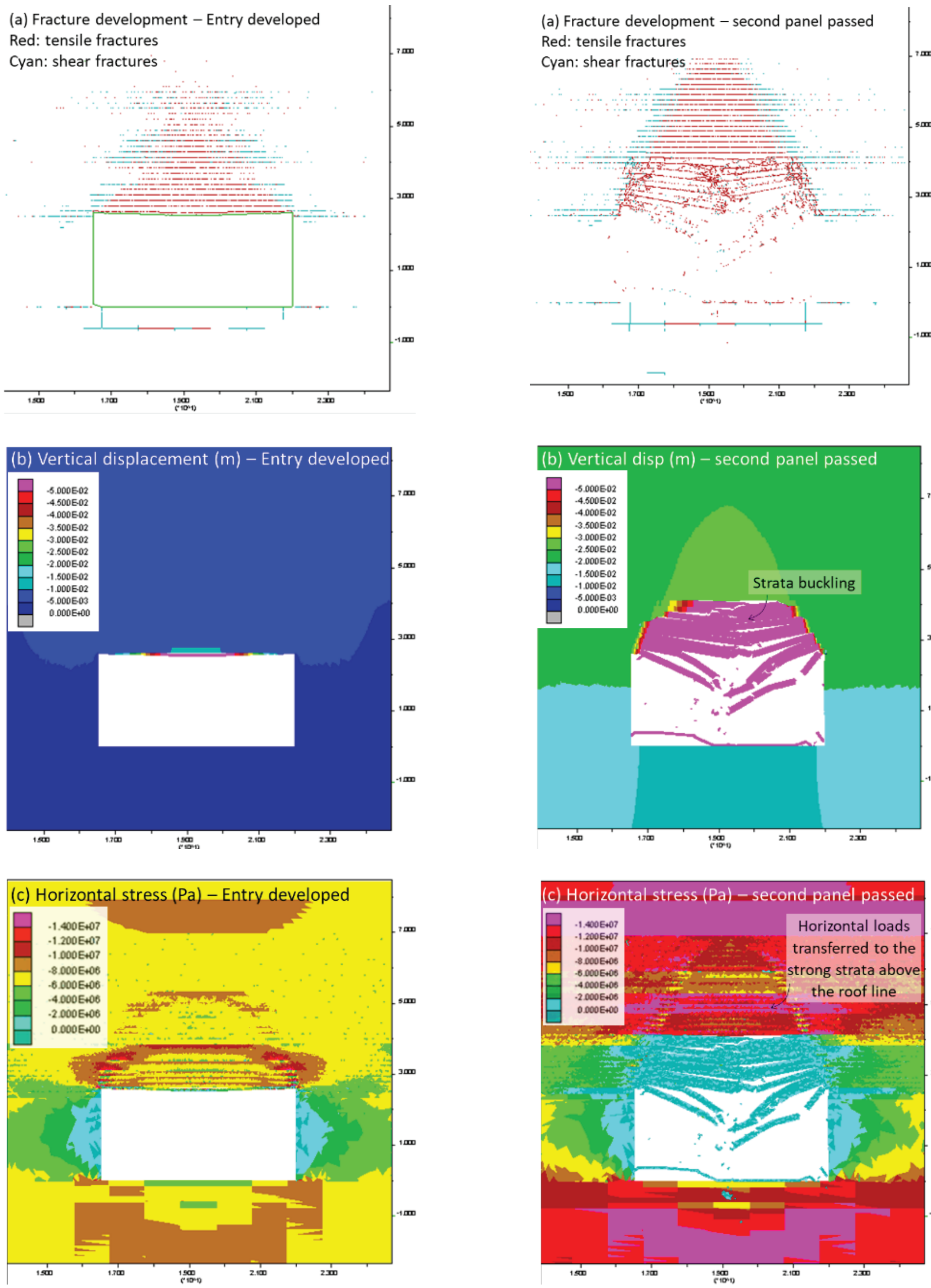

(a) Fracture development – Entry developed
Red: tensile fractures
Cyan: shear fractures
(a) Fracture development – second panel passed
Red: tensile fractures
Cyan: shear fractures
(b) Vertical displacement (m) – Entry developed
(b) Vertical disp (m) – second panel passed
Strata buckling
(c) Horizontal stress (Pa) – Entry developed
(c) Horizontal stress (Pa) – second panel passed
Horizontal loads
transferred to the
strong strata above
the roof line

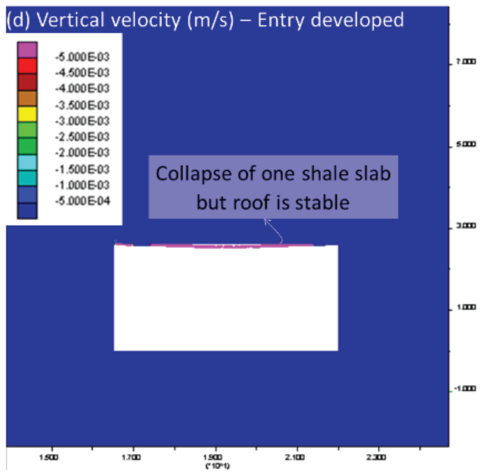

Figure 7. Model results showing entry response after development – no support

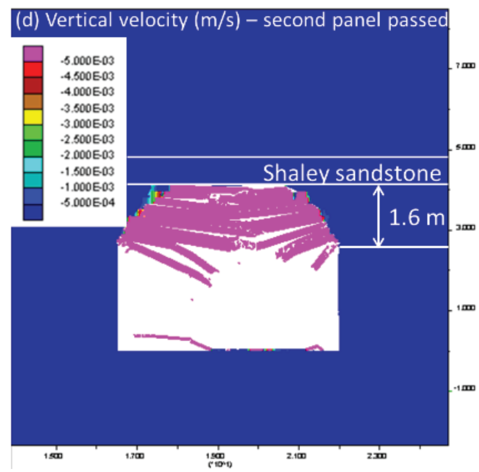

Figure 8. Model results showing entry response after the second panel reaches the monitoring site – no support

Figure 9a shows the horizontal stress within four delaminated shale slabs above the roof of the entry model without roof support. The first stage shows the development of the entry that is simulated by gradually reducing the reaction force on the entry boundaries in ten steps.

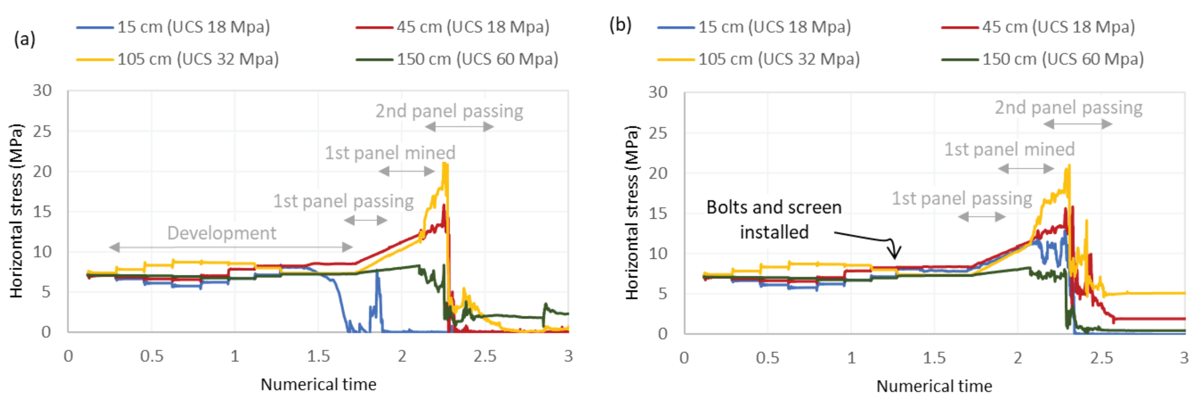

Figure 9. Horizontal stress recorded in the entry model at four points above the roof line at different stage of loading for (a) unsupported entry and (b) supported entry.

During development, the lower slabs (15 cm and 45 cm above the roof line) experience a reduction in the horizontal stress mainly due to the tensile stress driven by the downward bending of the strata. Consequently, the upper slabs are exposed to higher magnitudes of horizontal stress due to the compression caused by the buckling mechanism. Field-scale UCS of each slab is included in Figure 9a, showing that each slab fails under horizontal stresses lower than their expected strengths. This shows that the main mechanism for entry roof collapse is probably shear or buckling of the delaminated slabs.

Entry Model Response with support

The same loading process is repeated in the entry-scale model in Figure 4 but this time the grouted bolts and cable bolts are installed at the 7th step of the initial entry unloading phase, as shown in Figure 9b, followed by a roof screen installation. The roof screen is modelled as an array of upwards forces on the roof to simulate a load capacity equal to the weight of the first slab. The grouted and cable bolts are modeled with cable elements in UDEC with 6 and 10 segments, respectively. The input mechanical properties for the bolts follow values used by Esterhuizen, et al. 2019.

Note that the same roof slabs in Figure 9a show the sign of yielding in Figure 9b but their residual strengths reinforced by the installed support continue to carry loads even after yielding. The model results after the entry development and when the second panel passes the site are shown in Figure 10 and Figure 11. Comparing Figure 10 with Figure 7, the local collapse of the first slab is controlled by the screen installed but the stress and fracture patterns are almost the same. Comparing Figure 11 and Figure 8, however, shows how the support system helps the roof strata maintain their strength by providing confinement to the slabs.

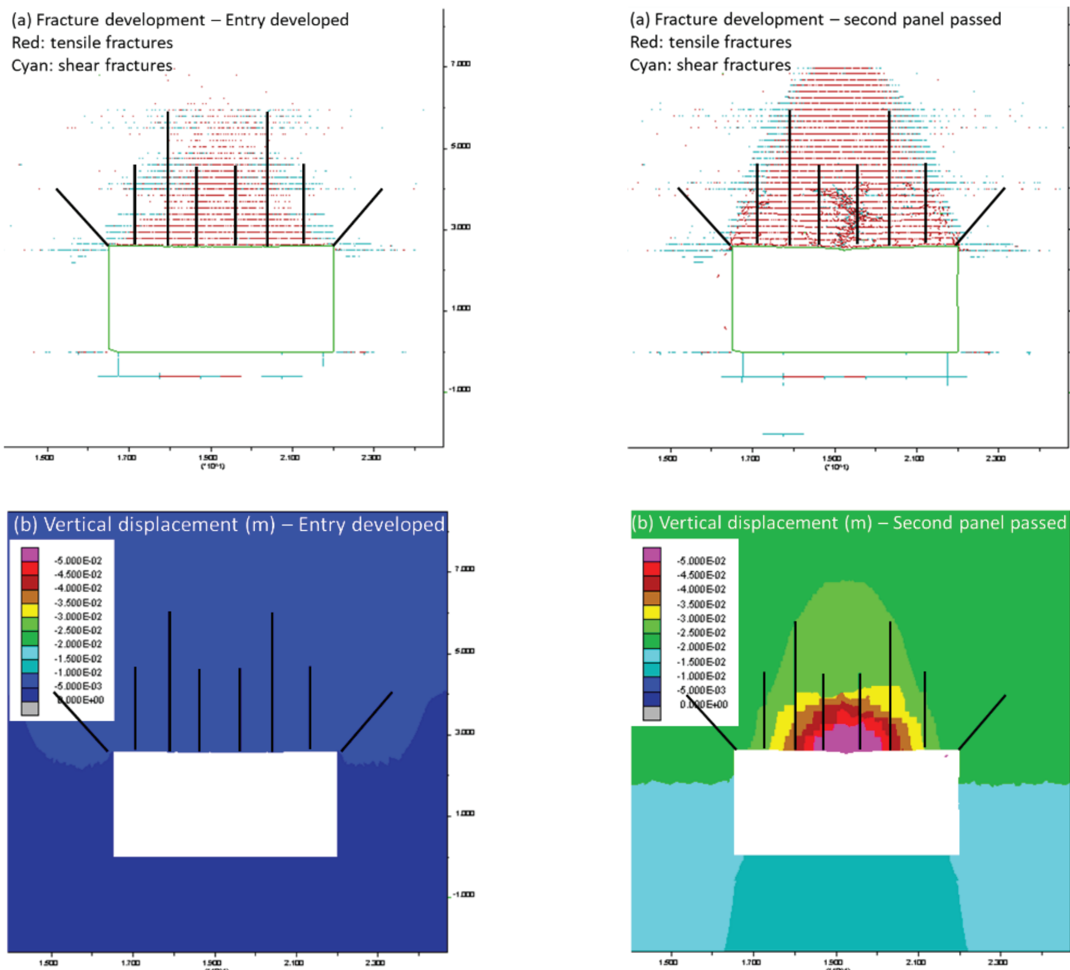

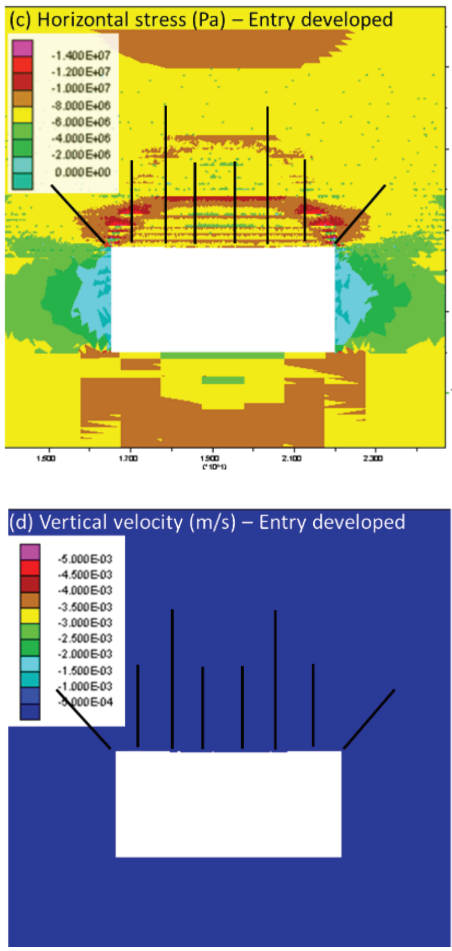

Figure 10. Model results showing entry response after development –*supported*

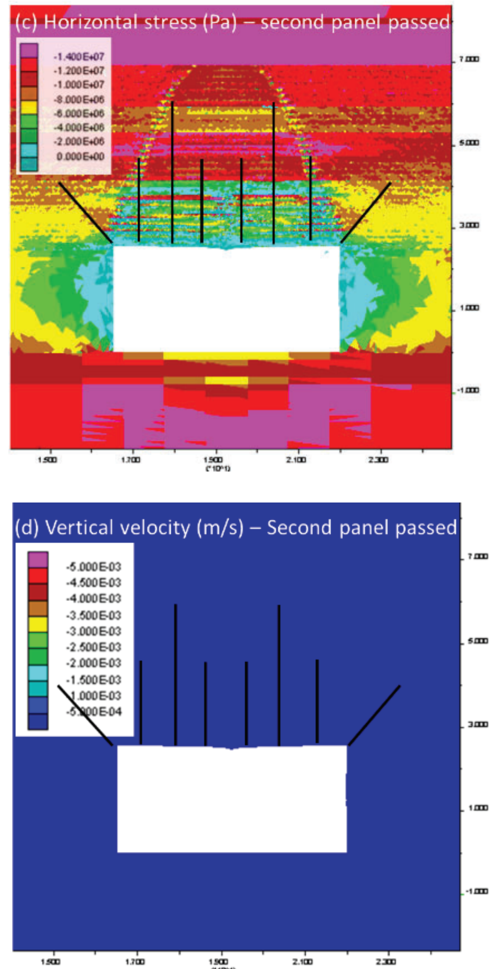

Figure 11. Model results showing entry response after the second panel reaches the monitoring site – *supported*

Figure 11a shows the fracture patterns stay almost the same with roof delamination extending up to more than 5 m above the roof line. The coal ribs show signs of yielding, and the floor has yielded, which is responsible for the limited floor heave observed at the site. Figure 11c shows how the stress bearing capacity of the first 1 to 2 m of the roof is reduced and stress is mainly transferred to the stronger middle and upper units in the roof. Finally, Figure 11d confirms that despite the roof sagging more than 5 cm, the roof is stable as observed in the field. Figure 12 shows the roof vertical displacements in the model up to a point 6 m above the roofline in the location of the roof extensometer shown in Figure 4.

Figure 12a shows the roof vertical displacements at the left and right-hand sides of the entry roof, showing the values predicted by the model and measured at the site. Figure 12b shows the vertical displacements at the center of the roof. The modeling results in Figure 12 overall show reasonable agreements with the extensometer results. The agreement between the modeling results and ground response shows the applicability of BBM in studying gateroad stability and paves the way for future analyses of support system alternatives under similar conditions.

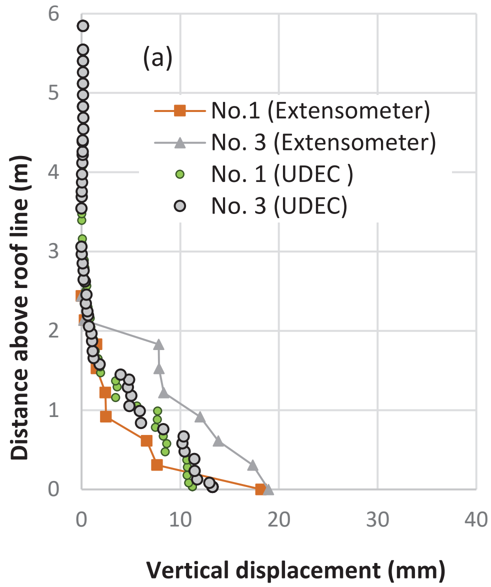

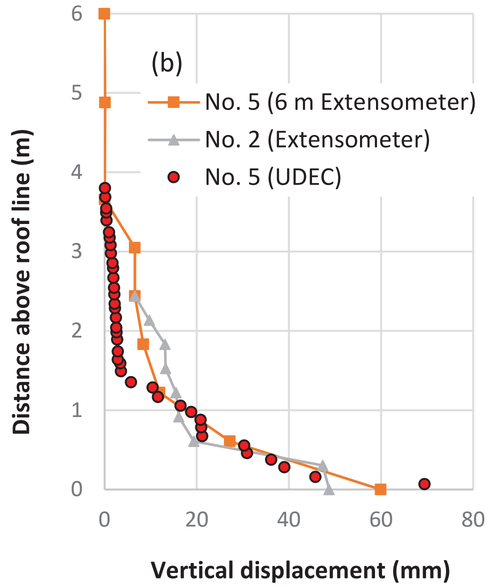

Figure 12. Vertical displacement up to 6 m above the roof line from UDEC and field extensometers at (a) the No. 1 and No. 3 extensometer locations and (b) No. 2 and No. 5 extensometer locations in Figure 4.

CONCLUSION

This work is a part of an ongoing research program in NIOSH for developing validated numerical models of supported entries to evaluate support alternatives. The objective of this paper was to investigate the BBM modeling approach for analyzing stability of longwall gateroad entry roof. The hypothesis was that BBM can reasonably capture the anisotropic strength of the strata, the delamination and bucking of bedded roof and its interactions with the support system with no need for elaborate modification of the model materials to capture the anisotropic strengths. The field monitoring data including stress measurement and roof sag in a three-entry-system longwall mine in the eastern US was selected for this study. An entry-scale model was developed using BBM technique. Roof stability was investigated without a support system in place, showing the bending of delaminated strata as the main failure mechanism. Support systems were then installed and their interactions with the roof was shown as to how they help maintain the residual strength of yielded strata and stabilize the roof. The roof sag from the model was compared with the extensometer results at three locations across the entry roof with reasonable agreement. These observations pave the way for further evaluation of the BBM modeling technique and its application to gateroad support design in different geological settings and stress conditions.

DISCLAIMER

The findings and conclusions in this report are those of the author(s) and do not necessarily represent the official position of the National Institute for Occupational Safety and Health, Centers for Disease Control and Prevention (CDC). Mention of any company or product does not constitute endorsement by NIOSH.

REFERENCES

Esterhuizen, G. S. 2012. "A stability factor for supported mine entries based on numerical model analysis." *The 31st international conference on ground control in mining.* Morgantown, WV: West Virginia University. 25.

Esterhuizen, G. S., D. Gearhart, and I. B. Tulu. 2017. "Analysis of monitored ground support and rock mass response in a longwall tailgate entry." In: Proceedings of the 36th International Conference on Ground Control in Mining." Morgantown, WV: West Virginia University. 11.

Esterhuizen, G. S., D. Gearhart, T. Klemett, H. Dougherty, and M. Van Dyke. 2019. "Analysis of gateroad stability at two longwall mines based on field monitoring results and numerical model analysis." *International Journal of Mining Science and Technology* 35-43.

Esterhuizen, G. S., T.S. Bajpayee, J.L. Ellenberger, and M. M. Murph. 2013. "Practical estimation of rock properties for modeling bedded coal mine strata using the Coal Mine Roof Rating." *the 47th US Rock Mechanics/Geomechanics Symposium.* Alexandria, VA: American Rock Mechanics Association. 1634–1647.

Esterhuizen, G.S., C. Mark, and M. M. Murphy. 2010. "Numerical model calibration for simulating coal pillars, gob and overburden response." *the 29th International Conference on Ground Control in Mining.* Morgantown, WV: West Virginia University.

Gao, F. Q., and D. Stead. 2014. "The application of a modified Voronoi logic to brittle fracture modelling at the laboratory and field scale." *International Journal of Rock Mechanics & Mining Sciences.*

Gearhart, D., G. S. Esterhuizen, and I. B. Tulu. 2017. "Changes in stress and displacement caused by longwall panel retreats." *the 36th International Conference on Ground Control in Mining.* Morgantown, WV: West Virginia University. 313–320.

Hasenfus , GJ., and DWH Su. 2006. "Horizontal stress and coal mines: twenty-five years of experience." *International Conference on Ground Control in Mining.* Morgantown, West Virginia University. 256-267.

Huang, Fan , Jiayi Shen, Ming Cai, and Chaoshui Xu. 2019. "An Empirical UCS Model for Anisotropic Blocky Rock Masses." *Rock Mechanics and Rock Engineering* 3119–3131.

Khademian, Z., K. M. Ajayi, D. W. H. Su, G. Esterhuizen, and S. J. Schatzel. 2021. "Geomechanical Modeling of Mining-Induced Permeability: Implications for Potential Gas Inflow from a Sheared Gas Well." *40th International Conference on Ground Control in Mining.*

Molinda, G.M., and C. Mark. 1994. *Coal Mine Roof Rating (CMRR): A Practical Rock Mass Classification for Coal Mines.* Information Circular 9387. U.S. Department of the Interior, Bureau of Mines.

Rashed, G., Y. Xue, Z. Khademian, and M. Sears. 2022. "Ground-fall Accident Trends in Mining: 2010 to 2019." *Mining, Metallurgy & Exploration.*

Tulu, I. B., G. S. Esterhuizen, D. Gearhart, T. M. Klemetti, K. M. Mohamed, and D.W.H. Su. 2018. "Analysis of global and local stress changes in a longwall gateroad." *International Journal of Mining Science and Technology* 127-135.

Tulu, I. B., G. S. Esterhuizen, K. M. Mohamed, and T. M. Klemetti. 2017. "Verification of a Calibrated Longwall Model With Field Measurements." *the 51st U.S. Rock Mechanics/Geomechanics Symposium,.* San Francisco, California.

Tulu, I. B., G. S. Esterhuizen, T. Klemetti, M. M. Murphy, J. Sumner, and M. Sloan. 2016. "A case study of multi-seam coal mine entry stability analysis with strength reduction method." *International journal of mining science and technology,* 193-198.

Zipf, R.K. 2006. "Numerical Modeling Procedures for Practical Coal Mine Design." *the 41st U.S. Rock Mechanics Symposium.* Golden, Colorado: American Rock Mechanics Association. 1-11.